Influence of Inertia on Liquid Absorption into Paper Coating Structures

Joachim Schoelkopf, Patrick A. C. Gane, Cathy J. Ridgway, OMYA AG, Oftringen, Switzerland and G. Peter Matthews, University of Plymouth, UK

Keywords : Inertia, absorption, imbibition, coating structures, porosity, liquid distribution, Lucas-Washburn, ink tack.

SUMMARY

We elucidate in this paper the influence of inertia of the imbibing liquid with special attention to the printing of paper. This is used to explain the observed differences between the absorption properties of fluids into large and small pores in paper coating structures. Without invoking arbitrary changes of the assumed constants in Lucas-Washburn (Washburn 1921) it has been hitherto impossible to describe the retarded imbibition seen when absorbing into highly porous structures containing large pores, for example in matt papers or coatings derived from very steep particle size distribution pigments.

We verify the differential effect between coarse and fine pores in a network model by the computational network simulator Pore-Cor where, uniquely, Bosanquet's equation (Bosanquet 1923), which describes both inertial and viscous capillarity, was incorporated together with mass balance calculations at each feature entry on a timestep of 1 ns. We apply the findings to compressed coating pigment samples of different porosities determined independently by mercury porosimetry. This is used to demonstrate the sensitivity of absorption rate and potential for separation of fluid(s) into differential pore sizes based on viscosity, fluid density and pore size distribution determined by the proportion of fine pores present up to a size equal to a Bosanquet-defined optimum. In a network, like a porous paper coating layer, it is proposed that for low viscosity wetting fluids the smaller features continue to fill sequentially according to this inertial preference to the initial exclusion of larger pores. The proportion of excluded pore volume after imbibition is a function of the available fluid volume which, to define this regime, must be less than the total available pore volume of the sample.

ADDRESSES OF THE AUTHORS:
Joachim Schoelkopf, Patrick A. C. Gane, Cathy J. Ridgway, OMYA AG, CH 4665 Oftringen, Switzerland.
G. Peter Matthews, University of Plymouth, Department of Environmental Sciences, Drake Circus, Plymouth, PL4 8AA, UK

Introduction

The investigation of the dynamics of fluid imbibition has stimulated researchers of different disciplines since the beginning of science. In a large number of cases the Lucas-Washburn equation (Washburn 1921) is used to describe the rate of imbibition or to determine the effective free surface energy of the solid phase structure. The term "effective" is in fact often used to overcome the lack of constancy of measurable parameters during the application of the Lucas-Washburn equation. In most cases it is argued that the contact angle during imbibition is deviating from the measurable quasi-static contact angle or the pore radius is adjusted arbitrarily to fit the experimental results. We show, however, that even when keeping the surface chemistry and pore morphology constant by simply changing the porosity through sample compression, Lucas-Washburn fails to scale the imbibition directly with pore size and the assumed constants are therefore forced to change.

It can be observed that despite the presence of big pores, associated with highly porous paper surfaces, liquid is absorbed observably slower than when fine pores are present (Gane, Hooper 1989; Bown et al. 1988). This also cannot be explained using the Washburn equation. This behaviour has also been described in the case of an ink (a suspension of solid particles in a fluid phase) (Xiang, Bousfield 1998). An ink-on-paper printing application could be physically described as a process of imbibition of a finite amount of liquid into a porous structure (paper) in competition with a contacting porous network formed by the drainage of fluid from that concentrating network (ink).

The rate of offset ink tack increase is a common measure of ink solvent removal by the paper and the subsequent ink curing (Gane et al. 1994). More recently, ink particle and dye deposition have also been studied, mainly related to ink jet applications, considering chromatographic separation of the ink (Chapman 1997). Of practical interest is the question how fast the liquid phase of the ink is absorbed and what are the contributing parameters and how are they controllable. In earlier work we described our approach including experiments of droplet imbibition to study the competitive mechanisms of relative pore filling and contrasted them to super source experiments to investigate the filling mechanisms varying between meniscus movement and potential film flow. In practical printing applications, other factors are present which contribute to the initial wetting dynamics, such as the pressure impulse transmitted from the printing blanket or roll through the fluid onto/into

the imbibing substrate. Linked also to compression is the spatial viscoelastic deformation of the porous network itself by the impact of pressure and heat changing the geometric parameters of the void structure itself. Furthermore, the Laplace pressure across the meniscus of the ink droplet (Marmur 1988), the geometry of the solid/liquid interface (Kent, Lyne 1989) (from nano- to macroscopic features) and the surface chemistry determine the contact angle, θ, of the three phase confluence. Despite the role played by these various factors, it is essential to begin with a convincing model for the observed unperturbed imbibition before embarking on including them with assumptions about their effects.

In the following we discuss the mechanism of inertial delay[1] of imbibition, which is due to the inertia of the liquid which resists the acceleration due to capillary forces and is especially dominant at short times and in large capillaries. Allied with this is the simultaneous phenomenon of inertial wetting which serves to accelerate the imbibition into finer pores. The network of a coating consists also of entry features throughout the structure forming a continuity of connectivity between the pore entities. Inertia must be considered at each of these entry features where accelerations are high - this is a key issue of our paper. Furthermore, it is well described that the liquid front in an inter-particulate void structure does not move evenly but in a jump-like behaviour when the dimension of the voids exceeds the meniscus continuity of a capillary, known as the Haines jump (Haines 1927). We confirmed this phenomenon under a light microscope observing dyed linseed oil imbibing into a SiO_2 particle structure. The micromechanics of the liquid jumps has been analysed and correlated elsewhere with pore geometry (Lu et al. 1995) and linked to liquid meniscus deformation (Sell et al. 1986; Sell et al. 1984; Maisch et al. 1981). It is obvious that each jump means strong acceleration. Therefore, in contrast to an idealised infinite straight capillary, where inertia acts only over a very short initial timescale, in an inter-particulate structure rapid acceleration happens repeatedly due to a number of potential phenomena and sums up to a deviation from Washburn behaviour.

[1] Inertial delay is not to be confused with the so-called wetting delay often seen on uncoated papers caused by surface molecular interactions such as arise from sizing where a low surface free energy barrier on the solid phase has to be gradually overcome by hydrative swelling.

Theory

We begin by considering the simplest case for the description of capillarity which is represented by an horizontal circular tube of definably small radius, *r*. The Laplace pressure *P* across the meniscus of a fluid in the tube describes the force of imbibition of the capillary and is given by the curvature of the liquid /gas (air) meniscus. To obtain an equation of dynamic motion the Laplace relation is traditionally incorporated into Poiseuille's equation of laminar flow: this was introduced by Lucas (Lucas 1918) and Washburn (Washburn 1921) and they obtained the well-known relation

$$x^2 = \left(\frac{rt}{2\eta}\right)\gamma_{LV}\cos\theta \qquad [1]$$

where *x* is the distance travelled by the liquid front in the hypothetical horizontal capillary, *r* is the capillary radius, *t* is the time, η is the dynamic viscosity, γ_{LV} the liquid-vapour interfacial tension and θ is the contact angle.

Equation *[1]* has some major drawbacks. Even in simple tube experiments, as schematically depicted in Fig. 1, there is much uncertainty about the dynamic contact angle (12), (numbers in brackets refer to Fig.1), and the exact meniscus shape (8) which are related to the condition of the tubelet inner surface in terms of microroughness (10,11), cleanliness, precursor development and prewetting conditions (9), which can be anything from a fluid monolayer to a bulk film and meniscus distortions due to "fountain" flow close to the wetting front (7). The dynamic effects at the entrance region (1-5) are also considered to be of similar complexity.

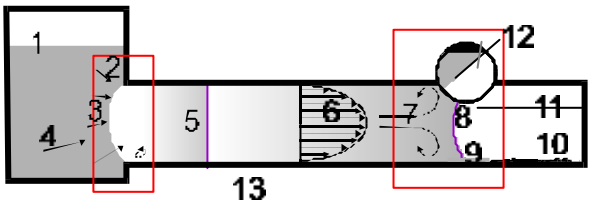

Fig. 1 *Overview of influences on meniscus-driven imbibition from a reservoir (left) into an empty capillary tube.*

In a porous structure, where a complicated spatial geometry merges with interconnectivity and sometimes surface chemical heterogeneity this uncertainty is yet more extensive. Therefore, the empirical equation

$$x^2 = kt \qquad [2]$$

of Bell and Cameron (Bell, Cameron 1906), is macroscopically just as valid as the most complex of any later derivations for a porous substrate.

Assuming that $\theta = 0$, an effective hydraulic radius (EHR) can be calculated in the basic Washburn equation. This assumes a viscous flow only. Any mechanism beyond this, such as that explained in the field of soil science as film-flow (Bernadiner 1998; Lu et al. 1994; Pepeira et al. 1996), may lead to entrapped air and give an effective, but not necessarily intrinsic, value of r.

The main drawback of equation *[1]* is the lack of inertial terms, relating to the mass of fluid under motion ((5) in Fig. 1) as recognised by Rideal (Rideal 1922). The practical relevance of inertia in capillary uptake was shown by Quéré using a high speed camera to detect the meniscus position in a small tube (Quere 1997). These phenomena may now explain why a mismatch is found as soon as the EHR approximation is compared to real structure data relating to percolation from mercury porosimetry. This mismatch led Li et al. to question the reliability of mercury porosimetry (Li et al. 1994). In contrast, far from questioning the reliability of mercury intrusion porosimetry, which has demonstrated its reliability if properly applied, we have tried to assimilate the dynamics of absorption to come to a better model.

We propose that the effect of inertia sums up at each single point within the porous network structure where acceleration is experienced by the liquid, probably at every relevant pore-throat connection. The resulting equilibrium macroscopic absorption behaviour may well in some cases also follow an $x \propto \sqrt{t}$ relation but not necessarily referring to the intrinsic factors in the Lucas-Washburn equation.

To account for inertia we incorporated a solution of the Bosanquet equation into a network model - the details of this work are given in a previous paper (Schoelkopf et al. 2000). Bosanquet complemented Rideal's solution in 1923 (Bosanquet 1923) adding the inertial impulse drag effect associated with an accelerating fluid, giving the following force balance:

$$\frac{d}{dt}\left(\pi r^2 \rho x \frac{dx}{dt}\right) + 8\pi\eta x \frac{dx}{dt} = P_e \pi r^2 + 2\pi r \rho g \cos\theta \qquad \textit{[3]}$$

where P_e is the external pressure, if applied, at the entrance of the capillary tube (1). By integration, and letting

$$a = \frac{8\eta}{\rho r^2} \qquad b = \frac{P_e r + 2\rho g \cos\theta}{\rho r} \qquad \textit{[4]}$$

it can be shown that

$$x_2^2 - x_1^2 = \frac{2b}{a}\left\{t - \frac{1}{a}\left(1 - e^{-at}\right)\right\} \qquad \textit{[5]}$$

where x_1 is the initial position and x_2 is the position after time t.

From equation *[5]*, it then follows that

$$x_2^2 - x_1^2 = b\,t^2 \qquad (at << 1) \qquad \textit{[6]}$$

If the measurement co-ordinates are set such that x_1 is zero and there is no applied external pressure P_e, then

$$x^2 = \frac{2\rho g \cos\theta\, t^2}{r\,\rho} \quad (at << 1, P_e = 0) \qquad \textit{[7]}$$

This equation describes what we refer to as 'inertial flow'. The distance travelled, x, is directly proportional to time t, in contrast to the Laplace-Poiseuille flow regime described by the Lucas-Washburn Equation *[2]* for which $x \propto \sqrt{t}$. Also in contrast, the distance travelled by inertial flow is independent of viscosity, but inversely related to the radius of the element r and the fluid density ρ.

The interesting practical question is, especially for a print process, whether inertia plays a role or not and if it can provide us with an explanation of the many contradicting predictions which are made by applying Lucas-Washburn alone. If the approximate pore radii of a porous surface and the printing ink vehicle densities and viscosities are in a mutual regime where inertia dominates we should determine at which time scale this happens and if it creates a differentiation in respect to the porosity actually sampled by the imbibing fluid. This becomes the target of the following sections.

Applying the theory

A brief compilation of the properties of some liquids relevant for ink composition and some model liquids used in the following computations is given in Table 1.

Table 1: *Overview of test liquids*

all data at ~20°C	Surface tension/ mN/m	Viscosity/ mPas	Density/ $kgm^{-3} \times 10^{-3}$	Potential Use
Water	72.75	1.056	0.998	Ink-jet/fountain-solution
1-Octanol	27.53	10.64	0.824	Flexo/Inkjet
Ethandiol	48.4	20.0	1.113	Flexo/Inkjet
Propandiol	45.8	57.1	1.053	Flexo/Inkjet
Butandiol	36.6	135.0	1.004	Flexo/Inkjet
Butantriol	55.9	1850.0	1.185	Flexo/Inkjet
Squalane	29.0	38.8	0.810	Offset/Roto
Nonane	22.85	0.71	0.718	Offset/Roto

To start the discussion we revert to the case of considering an idealised infinite capillary. Under the conditions of inertial uptake, the regime of equation *[7]* describes a monolithic block of fluid entering the capillary, driven by the wetting force of the liquid contacting the initial sidewalls. The fluid is assumed to have a flat meniscus front, except in practice at the actual wall contact, and all parts of the fluid within the capillary move at the same rate – hence the independence from viscosity. The flow is retarded more for a high density fluid entering a large capillary because the mass of fluid, and hence its inertia, is higher. Also, the higher the viscosity of the fluid, the faster the effect of viscous drag becomes apparent. This effect of inertial retardation and subsequent introduction of viscous drag is shown quantitatively for propandiol (viscosity 57.1 mPas) entering idealised capillaries with contrasting radii of 1 µm and 1mm, respectively, in Fig. 2.

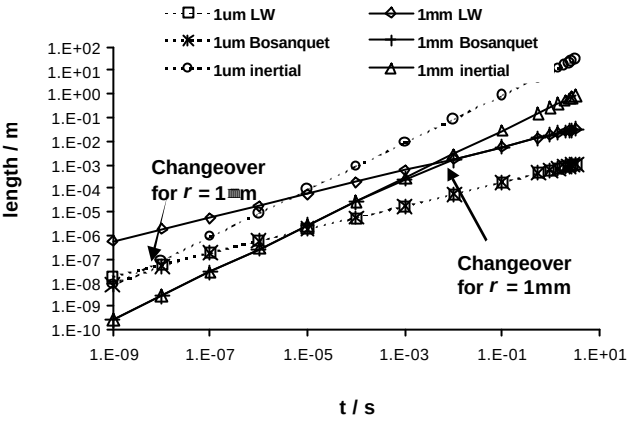

Fig. 2 *Comparison of inertial and viscous equations and Bosanquet's solution for propandiol and a simple straight capillary.*

The graphs show how the proposed (Bosanquet) flow changes from inertial to Lucas-Washburn (LW) flow as time and distance increase. For a capillary of 1mm radius, the change-over begins at about 0.01 s and after 1 mm penetration, and for a tube of 1µm radius it starts at about 0.01 µs and 0.1 µm absorption distance. For even smaller capillaries, the change-over will occur even faster and earlier, so that the fluid flow will be accurately described by the Lucas-Washburn solution in the finest of capillaries for supersource conditions. Also, with increasing fluid viscosity, whilst keeping density and radii constant, the change-over will occur earlier which shows that viscosity and radius are in a mutual relationship through frictional dissipation compared with the density and radius in turn determining inertia.

The comparison of Fig. 3 and Fig. 4 shows the difference in penetration depth, or filled wetting length in a capillary, predicted first by Lucas-Washburn and secondly by Bosanquet for nonane as a typical representation of mineral oil. We clearly see the pronounced influence of the liquid density in combination with growing radius promoting inertial retardation of uptake. The effect is even more strikingly visible when regarded as the predicted wetting front axial velocity as shown, for nonane, in Fig. 5 according to Lucas-Washburn and in Fig. 6 according to Bosanquet.

When regarding velocity we have to consider that neither equation strictly applies at time $t = 0$ because the acceleration of the fluid is not accounted for but rather its momentum. This effectively results in infinite acceleration at the origin. Nevertheless the velocities shown at $t > 0$ are reliably indicative.

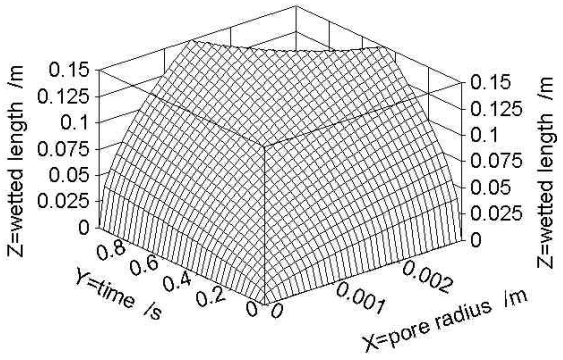

Fig. 3 *Nonane absorption length into a distribution of capillary sizes as defined by the Lucas-Washburn equation.*

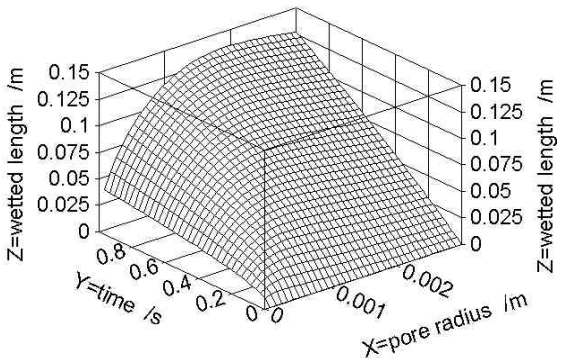

Fig. 4 *Nonane absorption length into a distribution of capillary sizes as defined by the Bosanquet equation.*

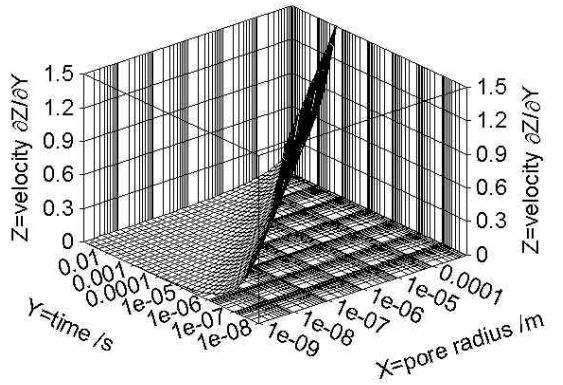

Fig. 5 *Nonane wetting front velocity entering an array of capillary sizes depicted by the Lucas-Washburn relation.*

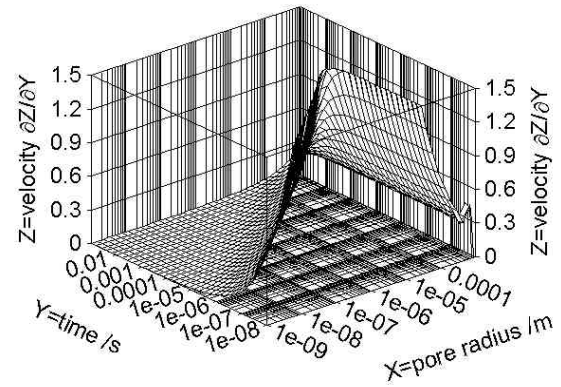

Fig. 6 *Nonane wetting front velocity entering an array of capillary sizes calculated from the Bosanquet equation.*

We see from the above plot (Fig. 6) that on the left side of the maximum velocity ridge, the viscous-Poiseuille regime applies, while on the right side (towards larger pore radii) the inertial, linear regime dominates. Therefore, we have to conclude that there exists a preferred capillary size which evolves as a function of time ranging from the finest at time $t = 0$ up to a given preferred size after time t defined by the Bosanquet "ridge" of maximum imbibition.

While these graphs demonstrate well the underlying physical effects, for practical printing situations maybe the most relevant form of these equations deals with liquid volume removal from the exposed surface. This case is depicted again for the low viscosity alkane (nonane) in Fig. 7 for Lucas-Washburn and Fig. 8 for Bosanquet, respectively.

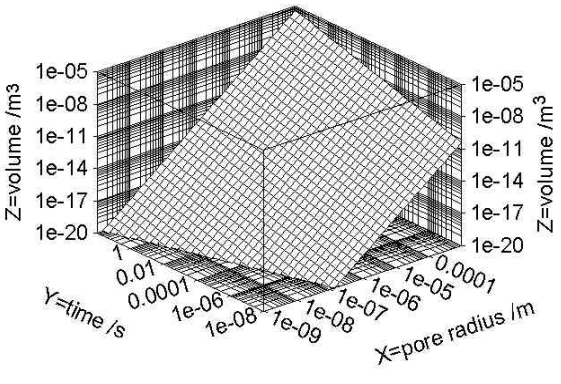

Fig. 7 *Volume absorption distribution in capillaries defined under Lucas-Washburn for nonane.*

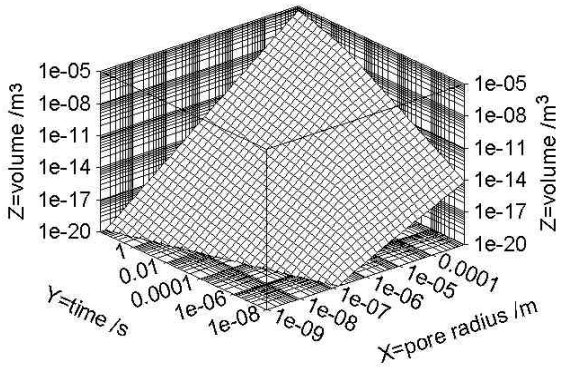

Fig. 8 *Volume absorption distribution in capillaries as defined by the Bosanquet equation for nonane.*

Under these newly-defined conditions it is important to understand how the absorption behaviour of a *network structure*, such as a paper coating layer, could be better understood and therefore made more controllable. We therefore now move from the idealised case of an infinite capillary to a network structure consisting of pores whose lengths are similar to their diameters, i.e. very short capillaries of progressively changing radius, joined by connecting throats. By changing the size distribution and geometry (or chemistry) of the pore network we view the fluid encountering a series of accelerations and decelerations as it reaches one the interconnecting throats. The dynamic equation of Bosanquet is then applied at each of these intersections such that inertial retardation and linear *t* absorption occurs depending on the capillary size.

As the name implies, a network model is an interconnected system of voids. Pore-Cor[2] is a computer model that simulates the void-space structure of porous materials based on an array of pores and connecting throats. It has been used to simulate the structures of a wide range of porous materials including sandstones, (Matthews et al. 1993), medicinal tablets, (Ridgway et al. 1997), and soil, (Peat et al. 2000). Pore-Cor uses a unit cell with 1000 cubic pores in a 10x10x10 array, connected by up to 3 000 cylindrical throats (i.e. one connected to each cube face). Each pore is equally spaced from its neighbouring pores by the 'pore row spacing' *Q*, and each unit cell is a cube of side length 10 *Q*. There are periodic boundary conditions: i.e. each cell is connected to another identical unit cell in each direction. The pore- and throat-size distribution of the unit cell is optimised so that the simulated percolation curve fits as closely as possible to the corrected experimental mercury intrusion curve, (Gane et al. 1995). The pore and throat size distribution is characterised by two parameters, 'throat skew' and 'pore skew'. The distribution of throat sizes is chosen to be log-linear. The throat skew is the percentage number of throats of the smallest size. The pore skew increases the sizes of the pores by a constant multiple. However, the pores with the largest sizes are truncated back to the size of the largest throat, thus giving a peak at the maximum size. The positions of the pores and throats are random, being determined by a pseudo-random number generator. The percolation characteristics of the network are insensitive to *Q*. Therefore, after convergence of the simulated percolation to the experimental percolation has been achieved by scanning through values of throat skew and connectivity, *Q* is adjusted so that the porosity matches the experimental value while ensuring that no pores overlap. It has been found that it is not normally possible to represent the complexity of the void network of a natural sample using the relatively simple geometry of a single Pore-Cor unit cell. Also, the size of the unit cell is often smaller than the representative elementary volume (REV) of the sample. Therefore, different unit cells must be generated using a different seed for the pseudo-random number generator. The model is designed so that different structural parameters in conjunction with the same seed of the pseudo-random number generator produce a family of unit cells which are similar to each other – for example, all may have a group of large pores in the same region. This aspect of the modelling is discussed in detail in a recent publication (Peat et al. 2000). Different stochastic generations use a different pseudo-random number generator seed, and can either use the original Pore-Cor optimisation parameters or can be re-optimised to the experimental data. The parameters and procedure are described in more detail in previous publications, (Matthews et al. 1995; Ridgway et al. 1997). Examples of the results of these two procedures for modelling pigment samples are given below.

The Bosanquet equation *[4,5]* is used to calculate the wetting flux in each filling throat in the void network of the model at every time step and the flux from the throats into an adjoining pore dictates the flow rate into that pore. Fluid subsequently exiting a filled pore into an adjoining throat that is not already filling from another pore is controlled by a mass balance with the influx into the pore. It is assumed that inertial flow occurs when fluid begins to enter each throat. At the start of the calculation of absorption the total time length for the process is specified. The length of a time step is 1 ns, its value being such that the maximum distance advanced by the fluid in one time step is never more than 0.1 *Q*

[2] Pore-Cor is a software program name of the Environmental and Fluids Modelling Group, University of Plymouth, Devon PL4 8AA, U.K.

whilst maintaining mass conservation requirements. The flow rate varies greatly with throat diameter, with the consequence that many millions of timesteps must be calculated. A typical calculation of absorption to fill one fifth of the unit cell takes 20 hours on a 600 MHz personal computer.

The absorption is quantified as F, the fraction of the total void volume which is filled with the fluid at time t. For comparison with experiment, the absorption is expressed as a Darcy distance $L = 10\ Q\ F$. This corresponds to the volume-averaged distance between the supersource in contact with the sample surface and the wetting front.

Slight maxima in the simulated absorption curves appear, (Fig. 9) due to the structural features of the individual Pore-Cor unit cells (Schoelkopf et al. 2000). The absorption of all stochastic generations was greater than that expected by the EHR approximation at times up to 0.1 ms. The Pore-Cor simulation predicted that the wetting occurred through many pathways into the unit cell, which could overtake many of the large voids, and therefore apparently wet more efficiently than predicted by a single, effective hydraulic stream tube. This, as we see later, produces the effect that was observed experimentally from droplet absorption tests (Gane et al. 2000) which we now go on to briefly review.

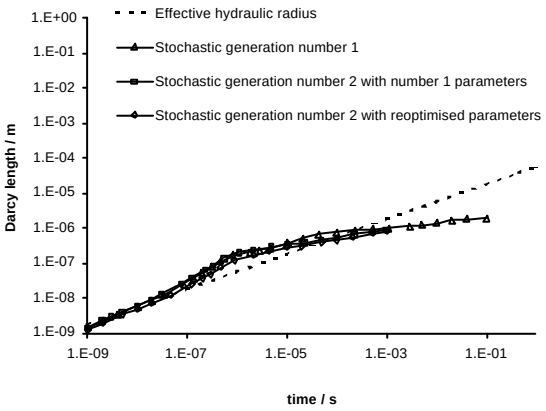

Fig. 9 *Simulations of absorption with Pore-Cor in the case of propandiol under Bosanquet.*

Materials and methods

In this section we refer briefly to the observations we made while testing the absorption volume distribution of dyed water droplets into compressed blocks of coating pigment over a range of controlled porosities (Gane et al. 2000). In that work we observed a transitional behaviour as porosity increased which was seen as an increase in penetration depth of the fluid as porosity increased up to a point where the depth of absorption once again decreased. This was analysed as a function of excluded pore volume, where the term excluded volume describes the pore volume that is not sampled by the imbibing fluid on the timescale and/or at the given available fluid volume for absorption.

To enumerate this deviation from complete pore filling/drainage, a simulation program was written calculating approximate dimensions of rotationally symmetrical oblate spheroidal segment volumes $V_{simdyed}$, using parameters obtained from the corresponding image analysis data of the absorbed fluid from a droplet test into a compacted tablet of calcium carbonate pigment and contrasting them to a theoretical dyed volume, $V_{theodyed}$, which would be given if all the pore volume were filled. By considering the applied volume of fluid and the tablet porosity, the degree of unfilled pores can be detected as the fractional excluded pore volume, $(V_{simdyed} - V_{theodyed})/ V_{simdyed}$, as shown in Fig. 10 as a function of porosity.

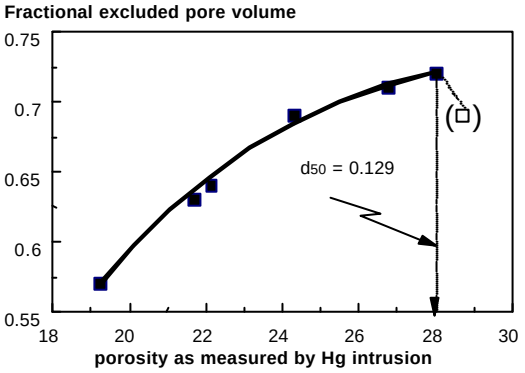

Fig. 10 *Fractional excluded pore volume ($V_{simdyed}$ - $V_{theodyed}$)/ $V_{simdyed}$ during droplet absorption as a function of measured porosity given in %.*

Discussion

Some possible mechanisms for this exclusion were discussed (Gane et al. 2000) and ranged from inhomogeneous surface chemistry within the pore network, geometrical divergence of the pore entry throats, surface creep and wetting phenomena associated with a retreating meniscus in strongly divergent pore geometries and finally competition

between fine and larger pores within the network due to some hitherto undefined absorption dynamic. Whilst not excluding any one of these potential mechanisms, we concentrate here, as mentioned before, on the probable effect of inertial retardation together with a new regime of inertial filling into fine pore features of the structure network as a model for pore size differentiation during absorption and leading to a preferential tracking of the fluid initially through a preferred network within the porous structure.

As we see from Fig. 10, the fractional excluded pore volume increases monotonically with increasing porosity until a maximum and then falls again. This indicates that if a competitive mechanism is to be proposed, that mechanism would have an increasing differential effect between pore sizes progressively favouring a given pore size or range of pore sizes until the proportion of that pore size once more decreased. If we consider Fig. 11, where we see the predicted pore radius differentiation for water, we see, as we did previously for nonane, that for this low viscosity fluid there is a maximum ridge on the projection of the 3D plot that runs from the finest pores at time zero and with an effective cut-off at a pore size equivalent to ~ 0.1µm after time ~ 10 ns. This acts progressively to favour a particular pore size region containing both the finest pores and all those pores up to a preferred equilibrium absorption pore size in competition with larger pores. This, in effect, is an integral of the available pores within a given pore size range which is determined by the fluid in question and the surface chemistry of the network solid.

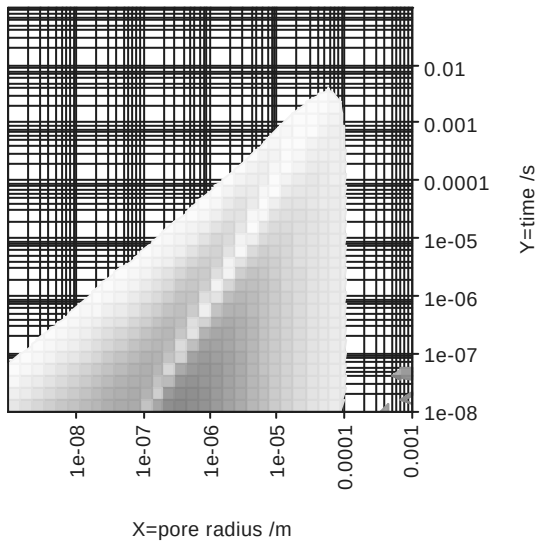

Fig. 11 *The decay of the "ridge" of maximum absorption velocity for water (bright shading on the z-axis projection) as a log/log/log plot - the base z-plane is 1ms^{-1}. The region from the origin to the point {0.1 µm, 10 ns} is taken as the preferred filling pathway.*

The choice of the time for absorption of ~ 10 ns for the cut-off on the axis of Fig. 11 is not arbitrary. If we consider the Bosanquet dynamic for water imbibing into pores we see that the effect of inertia is first of all directed toward the exclusion by retardation of all but the finest pores from the absorption process close to time $t = 0$. Then the effect of inertia is to favour absorption into those pores corresponding to the maximum in the Bosanquet surface which progresses away from the origin decaying in magnitude progressively with time. For water, the decay time is ~ 10 ns in a single pore. Now, we can correlate the maximum in observed exclusion from Fig. 10 in an actual experimental structure which had a measured median pore size of 0.129 µm (Gane et al. 2000). This value is close to the predicted pore size sampled preferably by inertial uptake after about 10 ns (~ 0.1 µm), i.e. the distance of absorption, if it were a capillary, is of the same order as the preferred pore size (Fig. 11). This in effect defines a predicted pore dimension of ~ 0.1 µm as being the maximum pore size, in the case of water, into which the inertial imbibition regime exists, thus giving a self-consistent agreement with experiment and providing the supporting evidence for modelling a network imbibition by preferential absorption into the integrated network volume consisting only of the finest pores up to and including a pore dimension of ~ 0.1 µm to the exclusion of the remaining pore volume. If we now consider that this mechanism applies at every junction of the pore network, the relevance of 10 ns in a capillary becomes extended to the time over which absorption occurs within the network, i.e. a summation of features all filling inertially with time steps up to 10 ns in each both simultaneously and sequentially to form the macroscopic observation of absorption. This is in stark contrast to the normally considered viscosity controlled regime which by this new model would only apply to cases of either much higher porosity containing no pores equal to or finer than the Bosanquet optimum or progression toward saturation in supersource (unlimited fluid volume) conditions.

In the case, therefore, for water absorbing into the Pore-Cor network model, shown in Fig. 12, it is successfully predicted that there is a progressive filling of the finer pores first followed by the larger pores. The progressive absorption can be followed visually from the software of the graphical model

itself as a function of time. Since there is a preferential distinction between pores up to a given preferred size, we can see that with limited volumes of fluid, not all pores will be filled within the volume defined by the penetrating front. Absorption progresses further into a wider range of pore sizes only after the initial inertial imbibition mechanism in each pore has subsided, which, in turn, then recurs at each accelerating feature in the network. Eventually, the energy is dissipated by viscous flow but still the front moves with the largest pores excluded even in this regime by the inertial retardation effect which continues to discriminate against the largest pores. The arrow in Fig. 12 highlights the furthest position of the fluid after an imbibition time of 10 µs.

We see also in Fig. 13 that a lower porosity structure, which means also a smaller mean pore diameter, doesn't show the preferred pathway effect to the same extent, primarily because there are not so many of the larger pores and throats present which are differentiated by inertial retardation.

We have shown, therefore, how the inertial effects can act within the network structure of a particulate porous material when the pore sizes and connectivity features are situated within the zone of sensitivity to inertial wetting behaviour. The calcium carbonate sample used in the referred study was brought into the threshold of this zone by applying compression to cover a range of porosities. By modelling these porous structures using Pore-Cor and applying the Bosanquet wetting algorithm the degree of excluded pore volume could be effectively evaluated.

For higher viscosity fluids (such as propandiol, butandiol and butantriol) we see from modelling that the finest pores, although beginning to fill, are quickly retarded by the higher viscous drag of these fluids resulting in potential exclusion of both the very finest and the largest pores. If saturation conditions were to apply then larger pores would have to be provided with fluid through a combination of absorption and percolation throughout the network as they could not compete against the capillarity of the finer pores.

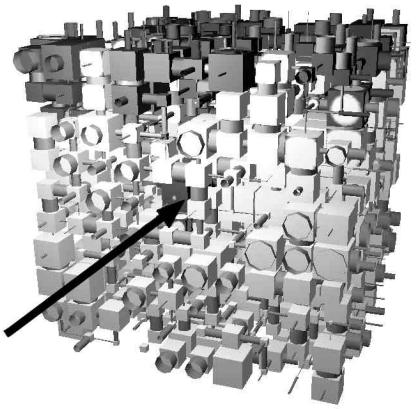

Fig. 12 *Schematic of a Pore-Cor cell filling under inertially controlled exclusion for water and a high porosity structure (F=28.02, Q=1.26µm)*

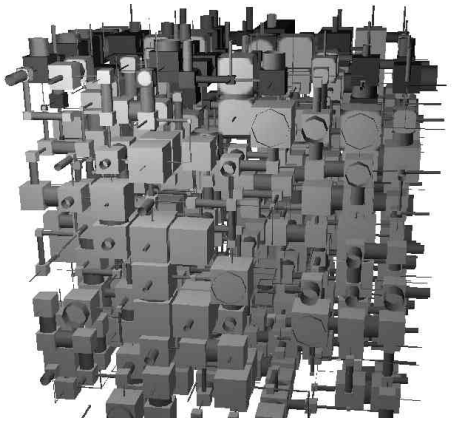

Fig. 13 *Schematic of a Pore-Cor cell filling under inertially controlled exclusion for water and a low porosity structure (F=19.26, Q=1.31µm)*

In the case of structures with only limited fine pores, this work shows that, practically, the removal of oils, for example, from an ink would remain incomplete as the fine structure in the drying ink acts to withhold fluid from the coating which now has insufficient remaining capillarity in the coating structure to complete the separation in competition with the fine pore structure and affinity remaining in the ink. The effects of meniscus and wall-wetting effects may become even more relevant for highly porous uncoated papers. The lack of "relevant" pore volume in an otherwise porous structure can only be explained through an effective exclusion mechanism such as we have discussed here.

There is increasing practical evidence for the exclusion phenomenon today in commercial papers, for instance, in the case of coarse pore structures in matt paper or gloss papers using very steep pigment particle size distributions. We can conveniently visualise this effect in the schematic shown in Fig. 14. In conjunction with the excluded volume we can predict qualitatively the effect of the exclusion mechanism on the observed tack cycle response of an offset ink as measured on a fresh printed ink film as a function of time. The general features predicted by this method, using the techniques described and discussed by Gane and Seyler (Gane, Seyler 1993; Gane et al. 1994), are in close agreement with this new model of absorption. Namely, the initial tack rise behaviour is controlled by the microstructure of the finest pores removing the low viscosity fluid phase, including some potential inter-polymer absorption phenomena by latex (Van Gilder, Purfeerst 1994), involving inertial exclusion of larger pores and absorption into the finest network up to and including the relevant Bosanquet optimum. This is followed by a slowing toward the maximum under the control of Lucas-Washburn absorption as viscous drag becomes increasingly dominant. Finally, absorption into the larger pores and latex interpolymer absorption during the longer time taken for surface tack to decay, leading toward complete ink drying, makes up the total pore volume as "seen" by the ink which finally samples some of the pores at first excluded on the shorter time scale but fails to sample those that have insufficient capillarity to compete with the forming internal ink pore network or those pores permanently excluded by retardation up to the volume of fluid available. Other features such as geometry or inhomogeneous surface chemistry may also lead to further excluded volume.

The problem of highly porous structures, or more particularly those with monosize pores, is seen by an almost endless surface tack effect indicating that some of the oil fractions remain in the ink. These circumstances of apparently anomalous "insufficient" pore volume, despite the use of highly porous coatings, are strongly implicated in poor post-tack ink-paper surface adhesion and the observation of poor ink rub resistance (Gane et al. 1994b).

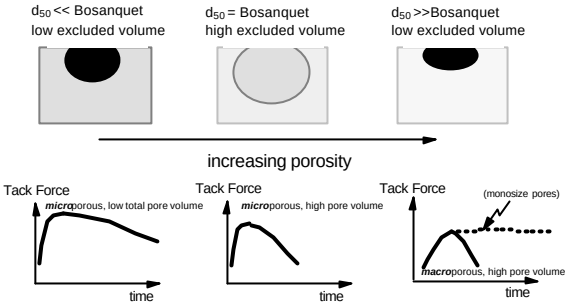

Fig. 14 *Schematic representation of the absorption steps controlling the tackification and surface drying of an offset ink.*

While the influence of spatial pore shape geometry is discussed elsewhere (Kent, Lyne 1989), the retarding influence of inertia may be controlled by adjusting the pore diameter distribution and surface chemistry distribution of the coating. This is increasingly being practised by introducing structured pigments and costructures between pigments of differing surface chemistry into the formulation of the coating colour (Gane et al. 1999).

The various exclusion mechanisms described provide interesting new opportunities to understand better how competition between fluids on grounds of their properties such as density and viscosity, as well as wettability, allows for various parts of pore structures to be filled differentially by these fluids. Perhaps we can begin to say why the apparently incompatible immiscibility of ink and water in the offset process actually works on a coated paper in that they can access either parts of the same void volume or differentiated pore volume in respect of not only wettability criteria but also pore size and absorption rate discrimination under the combined dynamics of network inertial imbibition, inertial retardation and viscous drag.

Conclusions

We have used observations from a simple droplet absorption method for the study of absorption of limited volumes of fluid into bulk samples of controlled porosity determined by mercury porosimetry. We have shown experimentally that there exists unfilled volume within the pore network volume defined by the wetting front as it is absorbed into a compressed pigment structure (Gane et al. 2000) and that this unfilled fraction increases as a function of porosity even when using a wetting fluid, i.e. the observed distance of absorption into a porous network of coating pigment is anomalously greater than would be expected if the total pore volume were to be filled.

This is contradictory to the prediction made by the simple Lucas-Washburn relationship which predicts that structures with large pores fill faster than those with fine ones and that all the pores in the highly porous structure would be expected to fill as the fluid front progresses. Under conditions of constant surface energy and wettability, pore diameter and geometry are shown to be the controlling factors. It is therefore necessary to search for a better imbibition model. The equation of Bosanquet, which includes an inertial term, indicates that there is a retarding force at the entry to large capillaries and an inertial wetting of very short fine capillaries. The viscous drag becomes established only over longer times in extended fine capillaries.

By extending inertial theory to a network model, it has been shown that absorption into a porous network proceeds preferentially by the finer pores in that network, at first by initial inertial imbibition together with exclusion of larger pores by inertial retardation, followed by viscosity-controlled Lucas-Washburn absorption dynamics but with the remaining inertial retardational exclusion of the largest pores. This inertially driven selectivity leads to the establishment of a preferred pathway during sequential filling.

Practically, for the papermaker and printer, this means that ink drying is predicted to be retarded on porous substrates containing few small pores or consisting of monosized pores before full equilibrium of complete pore filling of the coating structure is established. The formation in the remaining surface ink layer of a fine structure with high affinity will act to retain fluids within the ink once the selective “preferred” network in a coating is filled. This results in an apparently anomalous "insufficient" pore volume as "seen" by the ink as its fluid phase enters the coating structure, often observed as problems of print rub, incomplete ink setting and even sweat-back, and can be related to a lack of fine structure or an observed low affinity for absorption in the coating structure.

Acknowledgement

The authors wish to acknowledge the valuable assistance given by Dr. D. Spielmann, Omya AG, regarding the experimental methodology.

Literature

Bell, J. M., Cameron, F. K. (1906): "The Flow of Liquids Through Capillary Spaces", Journal of Physical Chemistry, *10*, 658.

Bernadiner, M. G. (1998): "A Capillary Microstructure of the Wetting Front", Transport in Porous Media, *30*, 251.

Bosanquet, C. M. (1923): "On the Flow of Liquids into Capillary Tubes", Phil. Mag., *S6 45*, 525.

Bown, R., Gane, P. A. C., Hooper, J. J. (1988): "Coating Thickness Analysis: an Evaluation of Interactions Between Coating Colour and Basepaper", Proceedings of the PTS Coating Symposium, Munich 1988, Wochenblatt fur Papierfabrikation.

Chapman, D.M. (1997): "Coating Structure Effects on Ink-Jet Print Quality", Proceedings of the 1997 Tappi Coating Conference, Tappi Press, Atlanta, 73-93.

Gane, P.A.C., Buri, M., Blum, R. (1999): "Pigment Co-Structuring: New Opportunities for Higher Brightness Coverage and Print Surface Design", International Symposium on Paper Coating Coverage, Helsinki, AEL METSKO, Finland.

Gane, P.A.C., Hooper, J.J. (1989): "Coating Profilometry: an Analysis of Coating Colour-Basepaper Interactions", Fundamentals of Papermaking, Transactions of the Ninth Fundamental Research Symposium; Mechanical Engineering Publications Limited, London, 871.

Gane, P. A. C., Kettle, J. P., Matthews, G. P., Ridgway, C. J. (1995): "Void Space Structure of Compressible Polymer Spheres and Consolidated Calcium Carbonate Paper-Coating Formulations", Industrial and Engineering Chemistry Research, *35*, 1753.

Gane, P. A. C., Schoelkopf, J., Spielmann, D. C., Matthews, G. P., Ridgway, C. J. (2000): "Observing Fluid Transport into Porous Coating Structures: Some Novel Findings", Tappi Journal, *85* , 1.

Gane, P.A.C., Seyler, E.N. (1993): "Some Aspects of Ink/Paper Interaction in Offset Printing", Proceedings of the PTS Coating Symposium, Munich 1993.

Gane, P.A.C., Seyler, E.N., Swan, A. (1994): "Some Novel Aspects of Ink/Paper Interactions in Offset Printing", International Printing and Graphic Arts Conference, Halifax, Nova Scotia, CPPA, Montreal, Canada, 209-228.

Haines, W. B. (1927): "Studies in the Physical Properties of Soils. IV. A Further Contribution to the Theory of Capillary Phenomena in Soil", Journal of Agricultural Science, *17*, 264.

Kent, H.J., Lyne, M.B. (1989): "Influence of Paper Morphology on Short Term Wetting and Sorption Phenomena", Proceedings of the 9th Fundamental Research Symposium, Cambridge, UK; Mechanical Engineering Publications Limited, London, 895-920.

Li, Z., Giese, R. F., Van Oss, C. J., Kerch, H. M., Burdette, H. E. (1994): "Wicking Technique for Determination of Pore Size in Ceramic Materials", Journal of American Ceramic Society, *77* , 2220.

Lu, T. X., Biggar, J. W., Nielsen, D. R. (1994): "Water Movement in Glass Bead Porous Media 1. Experiments of Capillary Rise and Hysteresis", Water Resources Research, *30*, 3275.

Lu, T. X., Nielsen, D. R., Biggar, J. W. (1995): "Water Movement in Glass Bead Porous-Media 3. Theoretical Analyses of Capillary Rise into Initially Dry Media", Water Resources Research, *31*, 11.

Lucas, R. (1918): "Ueber das Zeitgesetz des kapillaren Aufstiegs von Fluessigkeiten", Kolloid Z., *23*, 15.

Maisch, E., Renzow, D., Sell, P.-J., Walitza, E. (1981): "Benetzungskinetische Vorgange in Rohren unter simulierter Schwerelosigkeit", Zeitschrift fuer Flugwissenschaften und Weltraumforschung, *5*, 189.

Marmur, A. (1988): "Penetration of a Small Drop into a Capillary", Journal of Colloid and Interface Science, *122*, 209.

Matthews, G. P., Moss, A. K., Spearing, M. C., Voland, F. (1993): "Network Calculation of Mercury Intrusion and Absolute Permeability in Sandstone and Other Porous Media", Powder Technology, *76*, 95.

Matthews, G. P., Ridgway, C. J., Spearing, M. C. (1995): "Void Space Modeling of Mercury Intrusion Hysteresis in Sandstone, Paper Coating, and Other Porous Media", Journal of Colloid and Interface Science, *171*, 8.

Peat, D. M. W., Matthews, G. P., Worsfold, P. J., Jarvis, S. C. (2000): "Simulation of Water Retention and Hydraulic Conductivity in Soil Using a Three-Dimensional Network", European Journal of Soil Science, *51*, 1.

Pepeira, G. G., Pinczewski, W. V., Chan, D. Y. C., Paterson, L., Oren, P. E. (1996): "Pore-Scale Network Model for Drainage-Dominated Three-Phase Flow in Porous Media", Transport in Porous Media, *24*, 167.

Quere, D. (1997): "Inertial Capillarity", Europhysics Letters, *39*, 533.

Rideal, E. K. (1922): "On the Flow of Liquids Under Capillary Pressure", Phil. Mag., 1152.

Ridgway, C. J., Ridgway, K., Matthews, G. P. (1997): "Modelling of the Void Space of Tablets Compacted Over a Range of Pressures", Journal of Pharmacy and Pharmacology, *49*, 377.

Schoelkopf, J., Ridgway, C. J., Gane, P. A. C., Matthews, G. P., Spielmann, D. C. (2000): "Measurement and Network Modeling of Liquid Permeation into Compacted Mineral Blocks", Journal of Colloid and Interface Science, *227*, 119.

Sell, P.-J., Maisch, E., Siekmann, J. (1984): "Fluid Transport in Capillary Systems Under Microgravity", Acta Astronautica, *11*, 577.

Sell, P.-J., Maisch, E., Siekmann, J. (1986): "Experimental Study of Fluid Transport in Capillary Systems", Acta Astronautica, *13*, 87.

Van Gilder, R. L., Purfeerst, R. D. (1994): "Latex Binder Modification to Reduce Coating Pick on Six-Color Offset Presses", Tappi Journal, *77*, 230.

Washburn, E. W. (1921): "The Dynamics of Capillary Flow", Physical Review, *17*, 273.

Xiang, Y., Bousfield, D. W. (1998): "The Influence of Coating Structure on Ink Tack Development", PanPacific and International Printing and Graphic Arts Conference, CPPA,Canada, 93-101.